Journal of Engineering Research and Reports

11(3): 5-19, 2020; Article no.JERR.51997
ISSN: 2582-2926

Simulation and Optimization of Municipal Solid Waste Combustion: A Case Study of a Fixed Bed Incinerator

Arthur M. Omari[1*], John P. John[1] and Baraka Kichonge[2]

[1]College of Engineering and Technology, Mbeya University of Science and Technology, Mbeya, Tanzania.
[2]Department of Mechanical Engineering, Arusha Technical College, Arusha, Tanzania.

Authors' contributions

This work was carried out in collaboration among all authors. Author AMO designed the study and wrote the initial protocols. All authors performed the statistical analysis, managed the analyses of the study, literature searches, wrote the first draft of the manuscript, read and approved the final manuscript.

Article Information

DOI: 10.9734/JERR/2020/v11i317060
Editor(s):
(1) Dr. Ahmed Bdour, The Hashemite University, Jordan.
Reviewers:
(1) Kiran D. Devade, Savitribai Phule Pune University, India.
(2) J. Dario Aristizabal-Ochoa, National University of Colombia at Medellín, Colombia.
Complete Peer review History: http://www.sdiarticle4.com/review-history/51997

Original Research Article

Received 25 September 2019
Accepted 04 October 2019
Published 26 March 2020

ABSTRACT

In this study, a Computational Fluid Dynamics (CFD) technique was used to develop a model for the simulation and flow conditions of the incinerator. The CFD technique are based on subdividing the volume of interest, i.e., the combustion chamber (or other parts of the plant) into a grid of elementary volumes. The relevant equations of conservation (mass, momentum, energy) are then applied to each of those elements, after defining all inputs, outputs and boundary conditions. The resulting system is then integrated from start to finish, after introducing momentum, mass and heat transfer. The objective of the study was to evaluate and optimize the performance of locally available incinerators in Tanzania. The small scale municipal solid waste incinerator modelling was done by using a fluent solver. The case study of the existing incinerator at a Bagamoyo hospital in Tanzania was used as a model and the obtained values were compared with simulated results and other publications for validation. The design optimization using CFD techniques to predict the performance of incinerator showed the deviation of input air by 14%, the mass flow rate by 26.5%,

**Corresponding author: Email: mngoma2003@hotmail.com;*

the mass fraction of carbon dioxide by 10.4% and slight deviation of nitrogen dioxide and carbon monoxide. The study suggested removing the ash during the incineration process by using a moving grate mechanism to minimize the possibility of formation of NO_X. The study found the maximum mass flow rate capacity of incinerator to be 68kg/h with input air A_1 as 0.03639 kg/s, input air A_2 as 0.03046 kg/s and input air A_3 as 0.03409 kg/s. The findings indicated that as capacity is scaled up, the available momentum declines relative to the dimensions of the furnace.

Keywords: Municipal solid waste; incineration; optimization; CFD.

1. INTRODUCTION

Incineration optimization being the best design alteration process is a condition in which municipal solid waste (MSW) materials are heterogeneous in nature [1,2]. They are heterogeneous in size, shape and geometry [3] with low energy contents, high moisture and pollution source materials [4,3,5]. Incineration is a process of oxidizing carbohydrates present in solid waste to carbon dioxide and water [6,7]. The remaining elements present in the waste are oxidized to acid gases [8] and solid particles to the volume reduction of approximate 5% of their original volume [9]. The concept of waste-to-energy incineration continues to dramatically evolve as potential energy recovery for electricity production and greenhouse gas reduction approach through “waste-to-energy” technologies [10,11]. However, the physical and chemical interaction between particles during incineration complicates the process [12,13] with the flow performance being affected by two primary parameters namely geometry shape of incinerator and operational modes [14].

Certain needed parameters are explored so that the best measurable performances in the given conditions are known [15]. Incineration can cause pollution to environment if the input parameter, size and conditions are not optimized. The variation of designs and input parameters to obtain the optimum output results during incineration process cannot perform without affecting pollution to the environment [14,16]. The optimization process performed using simulation is preferred since it is faster and environmental friendly [17,18]. There are abundant of complex information and data being generated by simulation [4] and therefore designers of incinerators need to understand the characteristics of input and output parameters and conditions [19]. The understanding of inputs such as proximate and ultimate analysis values, type of waste, primary chamber and secondary chamber airflow and the output parameters such as temperature, flue gas, bottom and fly ash composition are important information for designers [20].

Optimization of operating conditions using Computational Fluid Dynamics (CFD) techniques is considered as economical [21] and flexible [22,23]. CFD is a popular approach that has been used to model, simulate and optimize MSW incinerators in a number of studies [4,24,25,26]. CFD is therefore very useful for visualizing some cardinal aspects of the combustion chamber, i.e., the fluid flow field (flow vectors, indicating flow direction, and rate in each point), temperature and pressure field, and combustion rate field. Optimization considers the maximization of economic performance, minimization of environmental degradation and increase the operation efficiency [27,21]. The main disadvantage of simulation is the cost of preparing a model and sometimes the difficulties in understanding and interpreting the simulation results [28].

The incineration process undergoes drying, devolatilization and char gasification in the primary chamber [29]. The reactions that take place are heterogeneous in which solid waste react with staved air to gasify the waste [30]. The reactions that take place in the secondary chamber involve the burning of gasified waste with excess air to form carbon dioxide and water [17]. The high temperature and excess air in the secondary chamber enhance the complete combustion of gases and destroy the toxic gases formed during the incineration [31]. Modelling heterogeneous and homogeneous reactions require simplifications and building a set of governing equations [23]. These various complicated process such as combustion, radiations and multiphase flow, must be known to designers [32]. The incinerator two chambers are set with main reason that the primary chamber stays at low temperature and staved air in order to gasify the waste and minimize particulates to the secondary chamber [33]. The secondary chamber is set to admit oxidant in order to complete burn all gases generated at primary chamber [34] and destroy all incomplete

combustion products [14]. The gases generated at primary chamber include CO, CO_2, H_2, H_2O, CH_4 and trace of hydrocarbons [6]. The speed and quantity of air inlet at the chambers are used to increase or decrease a residence time in a primary or secondary chambers and therefore enhance combustion [32].

Conditions such as oxygen concentration, residence time, temperature and mixing turbulence has a big influence in the formation of pollutants [35]. The higher amount of CO in the exit is a sign of incomplete combustion [16,36]. The efficiency of an incinerator can be gauged by the concentration of effluent gases such as CO_2, O_2, CO, H_2 and NOx [37]. Poisonous gases released in the effluent can be identified by using CFD techniques [38]. In the current work, optimization of municipal solid waste combustion – a case study of a fixed bed incinerator is presented. CFD technique used to develop a model for the simulation and optimization of incinerator flow conditions.

2. MATERIALS AND METHODS

2.1 CFD Analysis and Technology

CFD is numerical analysis methods which solve fluid flow related to physical process and biochemical processes [39]. CFD results may lead to better designs, low risk during testing and faster in improving the designs [23,40]. CFD provides the necessary information on how the flow takes place in the incinerator [41]. The CFD techniques give a critical evaluation in design and operating performance [42]. CFD plays a role in reducing the time and technical risks during the designing process [22]. CFD technology is mainly divided into three major parts as follows:

i). **Pre–Processing**– It includes the conceptual design, meshing and the formation of the computational model.

ii). **Processing**– This follows after developing mesh, the series of solution for solving physical models. The input values are specified in CFD to solve the governing equations for each cell until convergence is achieved.

iii). **Post Processor**– Visualize and interpret the data generated by the CFD processing [43].

2.2 CFD Governing Equations

Narvier Stokes equations of fluid dynamics are the conservation law of mass, momentum and energy [44].

i) Conservation of mass for gaseous phase

$$\frac{\partial}{\partial t}\alpha_g\rho_g + \nabla\cdot(\alpha_g\rho_g\vec{u}_g) = \sum_{g=1}^{n}\dot{m}_{gs} \tag{1}$$

ii) Conservation of mass for solid phase

$$\frac{\partial}{\partial t}\alpha_s\rho_s + \nabla\cdot(\alpha_s\rho_s\vec{u}_s) = \sum_{s=1}^{n}\dot{m}_{gs} \tag{2}$$

iii) Conservation of momentum for gaseous phase

$$\begin{aligned}&\frac{\partial}{\partial t}\left(\alpha_g\rho_g\vec{u}_g\right)+\nabla\left(\alpha_g\rho_g\vec{u}_g\vec{h}_g\right)=\\&-\alpha_g\nabla_p+\nabla.\vec{\tau}_g+\sum_{g=1}^{n}\left(R_{gs}+\dot{m}_{gs}\vec{u}_{gs}\right)+\alpha_g\rho_g\vec{F}_g\end{aligned} \tag{3}$$

iv) Conservation of momentum for solid phase

$$\begin{aligned}&\frac{\partial}{\partial t}\left(\alpha_s\rho_s\vec{u}_s\right)+\nabla\left(\alpha_s\rho_s\vec{u}_s\vec{h}_s\right)=\\&-\alpha_s\nabla_p+\nabla.\vec{\tau}_s+\sum_{s=1}^{n}\left(R_{gs}+\dot{m}_{gs}\vec{u}_{gs}\right)+\alpha_s\rho_s\vec{F}_s\end{aligned} \tag{4}$$

v) Conservation of energy for gaseous phases

$$\begin{aligned}&\frac{\partial}{\partial t}\left(\alpha_g\rho_g h_g\right)+\nabla\cdot\left(\alpha_g\rho_g\vec{u}_g h_g\right)=\\&-\alpha_g\frac{\partial p_g}{\partial t}+\vec{\tau}_g.\nabla\vec{u}_g-\nabla\cdot\vec{q}_g+\sum_{g=1}^{n}\left(Q_{gs}+m_{gs}h_{gs}\right)+S_g\end{aligned} \tag{5}$$

vi) Conservation of energy for solid phases

$$\begin{aligned}&\frac{\partial}{\partial t}(\alpha_s\rho_s h_s)+\nabla\cdot(\alpha_s\rho_s\vec{u}_s h_s)=\\&-\alpha_s\frac{\partial p_s}{\partial t}+\vec{\tau}_s.\nabla\vec{u}_s-\nabla\cdot\vec{q}_s+\sum_{s=1}^{n}(Q_{gs}+m_{gs}h_{gs})+S_s\end{aligned} \tag{6}$$

vii) Conservation equation of the mass fraction of species *i* in the gaseous phase

$$\begin{aligned}&\frac{\partial}{\partial t}\left(\alpha_g\rho_g Y_g^{\,i}\right)+\nabla\cdot\left(\alpha_g\rho_g\vec{u}_g Y_g^{\,i}\right)=\\&\nabla\cdot(\alpha_g\rho_g\Gamma_g^{\,i}\nabla Y_g^{\,i})+S_g^{\,i}\end{aligned} \tag{7}$$

viii) The conservation equation of the mass fraction of species *i* in the solid phase

$$\frac{\partial}{\partial t}\left(\alpha_s \rho_s Y_s^i\right) + \nabla \cdot \left(\alpha_s \rho_s \vec{u}_s Y_s^i\right) = \nabla \cdot \left(\alpha_s \rho_s \Gamma^i \nabla Y_s^i\right) + S_s^i \quad (8)$$

***k-ε* Turbulence Model:** Turbulence kinetic energy, *k* and its rate of dissipation *ε* are obtained from the following transport equation [45].

$$\frac{\partial}{\partial t}(\rho k) + \frac{\partial}{\partial_{xi}}(\rho k u_1) = \frac{\partial}{\partial x_i}\left[\left(\mu + \frac{\mu t}{\tau_k}\right)\frac{\partial k}{\partial x_j}\right] + G_k + G_b - \rho \in -Y_m + S_k \quad (9)$$

and

$$\frac{\partial}{\partial t}(\rho \in) + \frac{\partial}{\partial x_i}(\rho \in u_i) = \frac{\partial}{\partial x_j}\left[\left(\mu + \frac{\mu_t}{\sigma \in}\right)\frac{\partial \in}{\partial x_j}\right] + C_{1\in}\frac{\in}{k}(G_k + C_{3\in}G_b) - C_{2\in\rho}\frac{\in^2}{k} + S_\in \quad (10)$$

Radiation Model [32,46]:

Radiation flux $$q_r = -\frac{1}{3(a+\sigma_s) - C\sigma_s}\nabla G \quad (11)$$

Where: a is the absorption coefficient; σ_s is the scattering coefficient, *G* is the incident radiation and C is the linear-anisotropic phase function coefficient,

$$\Gamma = \frac{1}{(3(a+\sigma_s) - C\sigma_s)} \quad (12)$$

From Eq. (12):

$$q_r = -\Gamma \nabla G \quad (13)$$

The transport equation *G* is

$$\nabla \cdot (\Gamma \nabla G) - aG + 4a\sigma T^4 = S_G \quad (14)$$

Where σ is the Boltzmann constant and S_G is a user defined radiation source.

Combining Eqs. (13) and (14), Eq. (15) can be obtained:

$$-\nabla \cdot q_r = aG - 4a\sigma T^4 \quad (15)$$

The expression $-\nabla \cdot q_r$ can be directly substituted into the energy equation to account for heat sources due to radiation [45]. The technical algorithm is shown in Fig. 1.

2.3 Model Description and Methodology

2.3.1 Geometry

The 3D incinerator geometry used in this study is depicted in Fig. 2. The incinerator geometry has a maximum width of 0.885 m, maximum depth of 1.195 m and maximum height of 4.043 m. The geometry is meshed and value of meshes is determined using Ansys fluent software and gives 1.67 m^3. The geometry of computational model was performed using the solid works v16 [47].

2.3.2 Meshing domain

The meshing geometry is converted to tetrahedral cells [48]. The cells were then converted to polygonal. The total converted cells were 83,406. The meshed incinerator design shown in Fig. 3.

2.3.3 Boundary and initial conditions

The converted polygonal cells were assigned a solver and boundary conditions [49]. The outflow, outlet-1 was assigned as pressure outlet, the 3-air inlet pipes were assigned as inlet-air A_1, inlet-air A_2 and inlet-air A_3. The boundary conditions for burners were assigned in which the primary chamber burner assigned as inlet burner B_1 and secondary combustion chambers burner as inlet burner B_2. The boundary condition for inlet door was assigned as inlet-door D_1.

2.3.4 Fundamental input parameters to the model

The input data to the model were generated by the experimental practice to feed in the model for simulation and optimization. The fixed bed incinerator has two chambers; the primary ignition chamber and secondary combustion chamber. There are two burners (B_1 and B_2) for primary and secondary chambers respectively. B_1 is inclined at an angle of 45° to the grate to enhance the swirling effect in the primary chamber. Three air inlets, inlet air A_1, inlet air A_2 and inlet air A_3 for supplying air to the primary and secondary chambers. Inlet air A_1 is located under fire bottom of the grate to supply staved air for primary chamber. Inlet air A_2 is located at the upper part of the primary chamber to supply the excess air for primary chamber. Inlet air A_3 is located at the secondary chamber for supplying excess air to the secondary chamber. The excess air that varies between 20 to 150% stoichiometry is suitable for combustion of

municipal solid waste [50]. The increase in excess air may lead to reduce the temperature of combustion chamber, which may result in unwanted effluents. In this work, the excess air is set in such a way that the sufficient air is obtained for complete combustion.

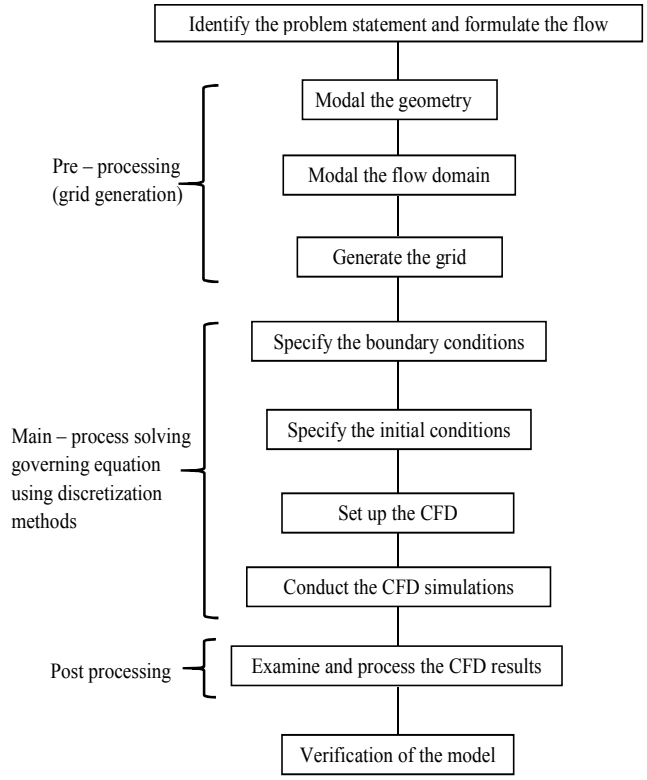

Fig. 1. CFD analysis process according to Ayaa [47]

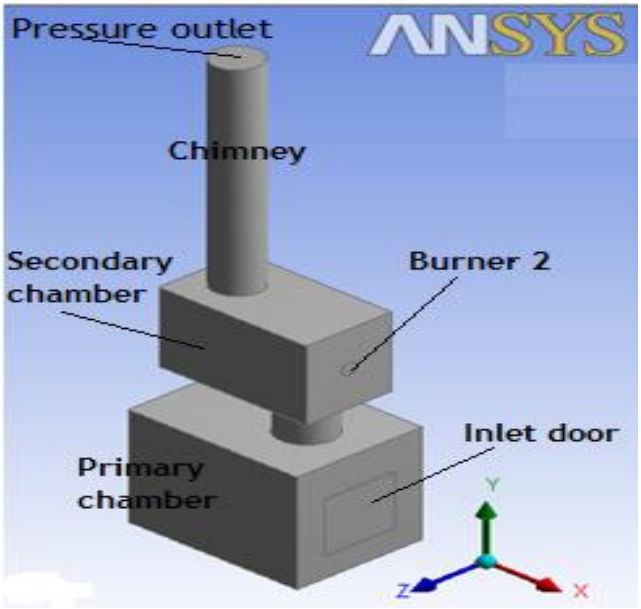

Fig. 2. Incinerator geometry

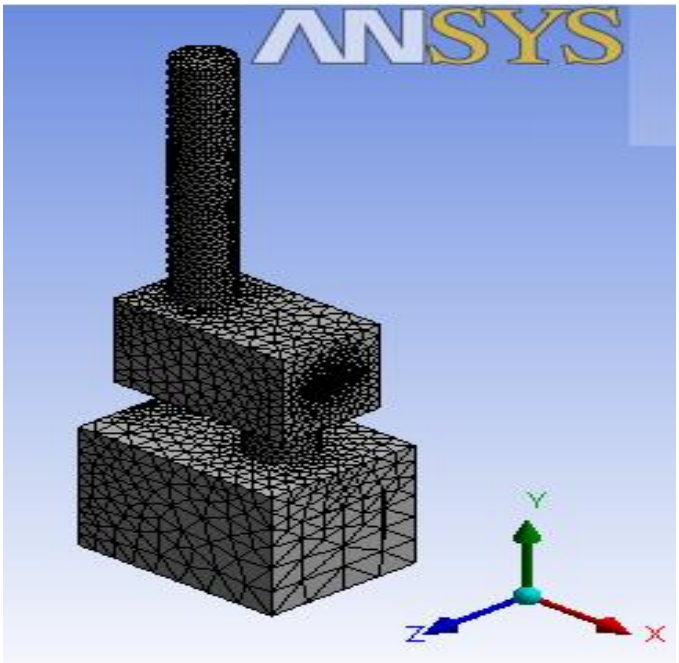

Fig. 3. Meshed incinerator geometry

2.3.5 Modeling of chemical reactions

The empirical formula for municipal solid waste of Arusha was adopted [51]. The process of dying, pyrolysis and gasification are taking place in the primary chamber. Under control temperature and staved air to form syngas such as CO, H_2 and CH_4 [52]. The gases escape from the primary chamber to the secondary chamber where complete combustion occurs [53,54]. The products of complete combustion gases CO_2 and H_2O exit through the chimney to atmosphere. These chemical reactions for drying, devolatilization, tar cracking, methanation and combustion of these gases in a single step reaction are tabulated in Table 1.

Table 1. Chemical equations described using single step reactions

Process	Chemical Reactions	
i.) Drying	$H_2O_{(l)} \rightarrow H_2O_{(g)}$	(16)
ii.) Devolatilization	$C_6H_{10}O_4 \rightarrow 2.33CH_{2.92}O_{0.938} + 3.087C + 0.0272CH_4 + 0.233CO + 0.3298CO_2 + 0.6599H_2 + 0.9277H_2O_{(g)}$	(17)
iii.) Tar Cracking	$CH_{2.92}O_{0.932} \rightarrow 0.7288C + 0.1429CH_4 + 0.0613CO + 0.0677CO_2 + 0.741292H_2O_{(g)} + 0.432972H_2$	(18)
iv.) Methanation *(H_2 gasification)*	$C + 2H_2 \rightarrow CH_4$	(19)
v.) Char combustion	$C + O_2 \rightarrow CO_2$	(20)
vi.) Water gas shift reaction (forward)	$CO + H_2O \longrightarrow CO_2 + H_2$	(21)
vii.) Water gas shift reaction (reverse)	$H_2 + CO_2 \longrightarrow H_2O + CO$	(22)
viii.) Bourdard Reaction *CO_2 gasification*	$C + CO_2 \longrightarrow 2CO$	(23)
ix.) Water Gasification	$C + H_2O \longrightarrow CO + H_2$	(24)
x.) *CO* Combustion	$CO + \frac{1}{2}O_2 \longrightarrow CO_2$	(25)
xi.) *H_2* Combustion	$H_2 + \frac{1}{2}O_2 \longrightarrow H_2O$	(26)
xii.) *CH_4* Combustion	$CH_4 + 2O_2 \longrightarrow CO_2 + 2H_2O$	(27)

3. RESULTS AND DISCUSSION

3.1 The Input Air

The measured value were adopted from published data in international journal as a result of the study of operating conditions of incinerator done at Bagamoyo-Tanzania [55]. The input staved air inlet A_1 located at the bottom of the primary chamber is deviated by 13.532% and it changes its original value from 0.03147 to 0.03639 kg/s, as shown in Table 2. The value of oxygen is increased due to increase in municipal solid waste burned. The amount of oxygen need to increase so as to assist in the process of thermochemical oxidation process to convert the biomass substance into syngas [56]. Air inlet A_2 that supplies air to the primary chamber shows the deviation of 4.971%. It decreases its original value from 0.03197 kg/s to the simulated value of 0.03046 kg/s as shown in Table 2. The value of oxygen is reduced to a lower value however; this deviation is allowable for such calculations. The pipe for supplying air to secondary chamber $A_{3\text{-}1}$ has decreased its value to 0.03409 kg/s from its original value by 6.98% this may be caused by slightly increasing the excess air supplied during the experimental process [56,57]. The maximum value of oxygen needed for optimum combustion is iteratively determined by fluent solver which gives the actual value needed to 0.03409 kg/s [58].

3.2 The Input Municipal Solid Waste

The optimized value for municipal solid waste mass flow rate shows the deviations, the simulation value shows that the incinerator has a capacity to incinerate municipal solid waste 26.475% more that its designed capacity. The simulation results from fluent solver show that the maximum capacity for one cycle can be 68 kgs instead of 50 kgs currently used. Iterated input model parameters and the input experimental parameters are shown in Table 2.

3.3 The CFD Output Simulation Results

The CFD output simulation results and the experiment result are depicted in Table 3.

3.4 Velocity Magnitude

The maximum velocity at the exit of the incinerator is ranging between 2.79 – 3.49 m/s with average velocity of 3.14 m/s shown in Fig. 4. Velocity has a minimum value at the primary chamber and higher value at the secondary chamber. The formation of gaseous material at the primary chamber increases the velocity of gases. The O_2 concentration in the secondary chamber increases the velocity and residence time due to excess air supplied [59].

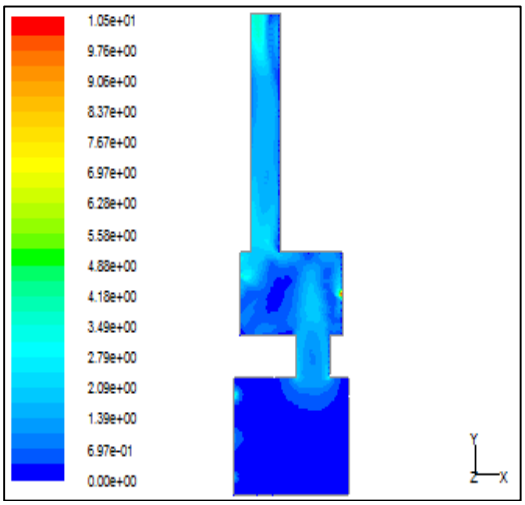

Fig. 4. Contours of velocity magnitude (m/s) (time = 1.6889e+01)

3.5 The Temperature of the Incinerator

The temperature inside the incinerator is shown in Fig. 5. The maximum temperature is 2400 K and the minimum is 300 K corresponding to room temperature and the feed-in temperature of municipal solid waste. The temperature is uniform in primary chamber, secondary chamber and in the chimney. The temperature at the secondary chamber is 1400 K and the average temperature of the chimney is about 1800 K but the core is 2000 K, ash is deposited at the bottom of the incinerator with a temperature of about 2400 K. The temperature at the entrance of pipe is high; this may be due to the excess air at that particular point. The excess air increases the combustion efficiency. The low heat zone at the bottom of the incinerator may be caused by insufficient air due to its position. Indeed, there is anomaly in the observed temperatures. A direct explanation to what is happening can be elucidated if further studies are carried in these areas. The temperature at the entrance of pipe is high; this may be due to the excess air at that particular point. The excess air increases the combustion efficiency. The low heat zone at the bottom of the incinerator may be caused by insufficient air due to its position. The temperature at the exit is about 1400 K. There

are two burners, which are located at primary and secondary chambers respectively. The ignition temperature of each burner is 480 K, which assists in increasing the temperature of the incinerator and support combustion for both primary and secondary chambers.

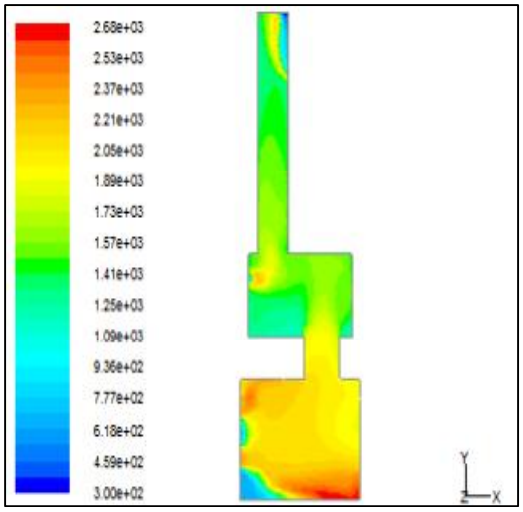

Fig. 5. Contour of static temperature (k)

3.6 Mass Fraction of Oxygen

The mass fraction for O_2 was decreased. The value of oxygen to the effluent is caused by excess air to the combustion process [60]. In this case, the value of oxygen to the practical experiment was exceeding as shown in Fig. 6 and Table 2. The increasing oxygen may cause this during the period of refilling the waste by opening the door of the incinerator, there is recalculated air from the entrance door.

3.7 Mass Fraction of CO Released

The simulation values for Carbon monoxide were deviated from practical values by 58.07% as shown in Fig. 7; this value is highly deviated. The percentage of Carbon monoxide increases as compared to practical results. The value is, however, within the permissible value of Carbon monoxide allowed in the environmental protection values [60]. This may be caused by the door opening in which excess oxygen to the combustion chamber is not considered during simulation.

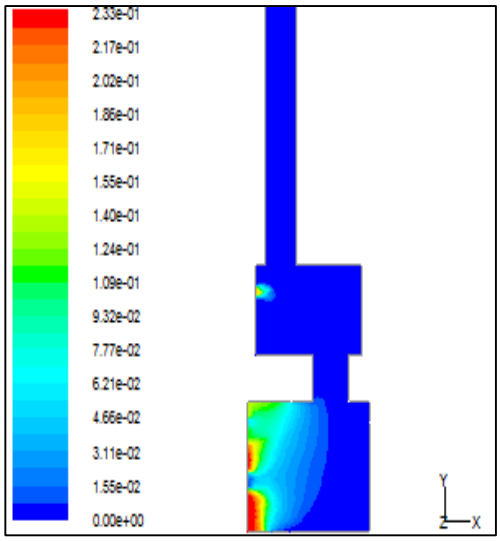

Fig. 6. Contour of mass fraction of o_2 (time = 1.1297e+01)

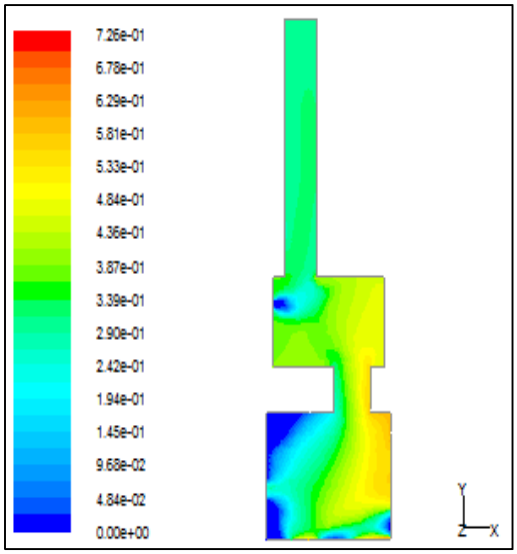

Fig. 7. Contour of mass fraction of CO (time= 1.1297e+01)

3.8 Mass Fraction of Carbon Dioxide Released

The values show that CO_2 released were deviated by 10.39% from the value obtained practically. The percentage CO_2 at the effluent gases was found to be 7.07%. The practical experiment obtained was 6.4% [55]. This variation is caused by increase in combustion efficiency of the incinerator [61,62].

Table 2. The comparison summary of input experimental parameters against simulation

Input mass flow rate				
Item	**Symbol**	**Measured (Experiment) (Kg/s)**	**Predicted (Kg/s)**	**Deviation (%)**
Door inlet	D_1	0.02778	0.03778	26.475
Staved air inlet	A_1	0.03147	0.03639	13.532
Primary excess air	A_2	0.03197	0.03046	4.971
Secondary excess air	A_3	0.03648	0.03409	6.98

Source: [55]

Table 3. Output parameters comparison

Parameters (mass fraction)				
Item	**Symbol**	**Measured (Experiment)**	**Predicted (Simulated)**	**Deviation (%)**
Velocity magnitude (m/s)	υ	4.0	3.75	6.25
Mass fraction of O_2 (%)	O_2	12.27	2.31	81.17
Mass fraction of CO (ppm)	CO	109.7	46	58.07
Mass fraction of CO_2 (%)	CO_2	6.4	7.07	10.39
Mass fraction of NO_x (ppm)	NO_2	152	372	144.74
Particle residence time (s)	t	2	1.73	13.5

Source: [55]

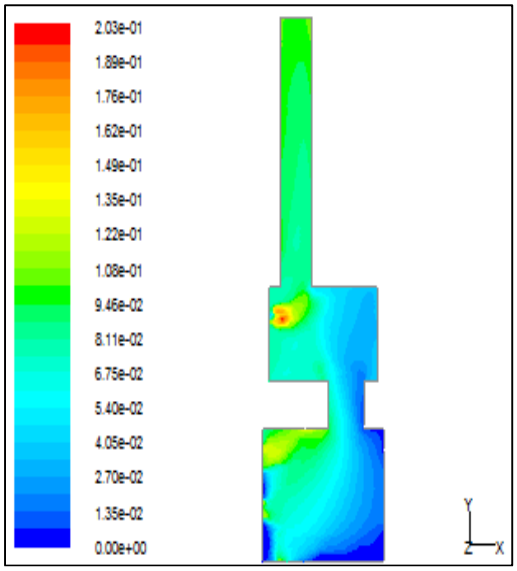

Fig. 8. Contours of mass fraction of CO_2 (time = 1.1297e+01)

3.9 Mass Fraction of NO_2 Emission (ppm)

The emission values for NO_2 deviated from practical values as shown in Fig. 9 and Table 3. The deviation values were 144.74%. This value is more than the practical values because some of the Nitrogen from air under high temperature forms thermal NO_x [63]. The increase the temperature of combustion may lead to the formation of more NO_x [64]. In the case studied, the highest concentration of NO_x was found to be at the bottom of the incinerator where the ash drops with high temperature are concentrated. This may be due to the high temperature of ash and excess air enters to the primary chamber during filling the waste while the combustion process continues. The ash concentration and the filling of waste during second and other higher cycles of operation may cause this excess temperature and excess air to form thermal NO_x which was not considered during the practical experiments [65].

3.10 The Particle Residence Time

The particle traces are coloured by residence time(s) as shown in Fig. 10. The particle residence time shows an average of 1.73s. These values correspond to various international standards for residence time such as Canadian standards which set the standard residence time to be not less than 1 second at a temperature not less than 1000°C [66]. The value of residence time influenced by the speed of inlet gases. The value of residence time is also affected by temperature and that is why at secondary chamber the residence time is lower than in primary chamber due to high temperature in a secondary chamber [41].

3.11 The Particle Path Lines

The particle traces represent the path. Initially a path was made by integrating the velocity with

time. For transient flow path is known as Pathlines. In this work, the Pathlines start from the boundary condition inlet A_1, inlet A_2, inlet A_3, inlet B_1, inlet B_2 and inlet D_1 and goes out through the outlet $_1$ as shown in Fig. 11. The results also show that there is a uniform flow of particles from bottom of the incinerator through the neck; then secondary chamber, the chimney to the exit. The detailed information of these pathlines contribute to the overall understanding of the flow of the particles [67].

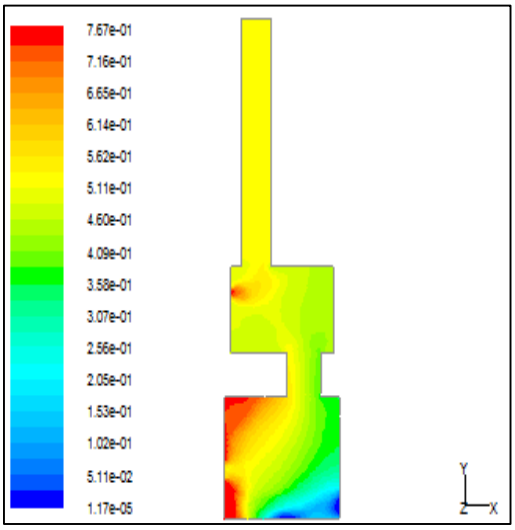

Fig. 9. Contours of mass fraction of NOx (time = 1.1297e+01)

3.12 Particle Diameters

The particle diameter decreased along the incinerator. The value of the particle diameter at the bottom is about 9.55e-04m while it decreases to 1.45e-04m just before the exit of primary chamber. At the secondary chamber there are very few particles and very small in size. Their diameter is about 1.0 e-04 m. The bigger particles remain in primary chamber and the very small particles pass through the neck, secondary chamber and chimney to exit. This separation of particles caused by two-chamber incinerator design in which the primary chamber solid particles gasified to combustible gases.

3.13 Average Temperature vs Incinerator Height

The average temperature is about 1400K at incinerator exit. The average temperature is increasing along the incinerator. The rapid change in temperature at 140 m is due to entering of gases from the primary chamber to secondary chamber. The temperature is gradually increased and reaches a maximum point at 210m. The temperature then fluctuates again between 1600k and 1400k to exit. The temperature at the chimney constant fluctuates between 1400 and 1600k. The fluctuation affected by the primary reaction in the combustion chambers.

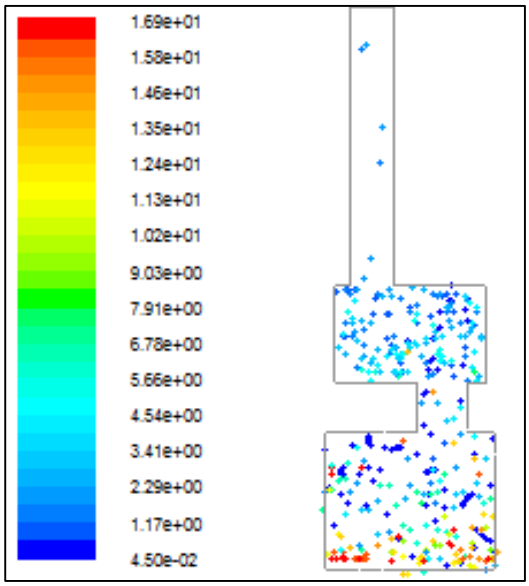

Fig. 10. Particle traces coloured by residence time(s) (time=1.6889e+01)

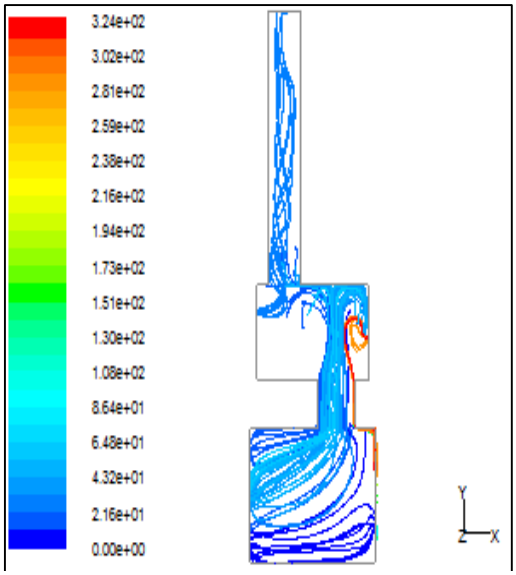

Fig. 11. Pathlines coloured by particle ID (time = 1.6889e+01)

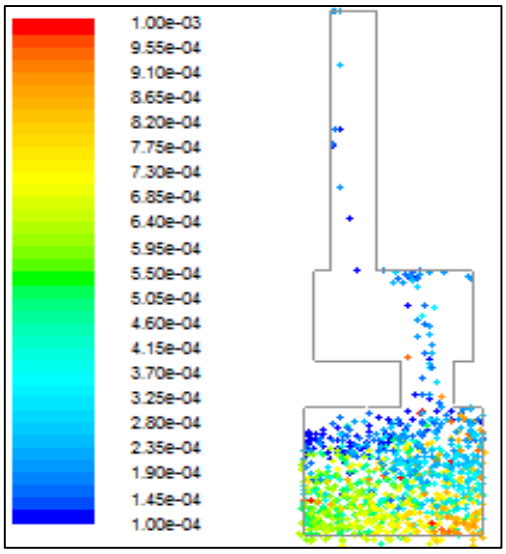

Fig. 42. Particle traces, colored by particle diameter (mixture) (m) time=1.4750e+00)

3.14 Average NOx at Incinerator Exit

Average NO_x is about 600 ppm at incinerator exit. This value is within the permissible value of NO_x gases, which react with oxygen to form acid rain.

3.14.1 CO_2 concentration

Comparison model result on the CO_2 obtained between current simulation and CO_2 obtained by [68] shows the results deviated by 36%.

3.14.2 NO_X concentration

For the case NO_X comparison between the current model results with those obtained by [68], shows the good agreement with deviation of 3%.

3.14.3 O_2 concentration

Comparison result obtain from the current model with [32] on O_2 concentration show the deviation of 33%, while the comparison between [69] show the deviation of 25%.

3.14.4 CO concentration

In the case of CO concentration, the findings from the current model with [32] shows the deviation of 32.2%, when compared with [69] model shows the deviation by 38%.

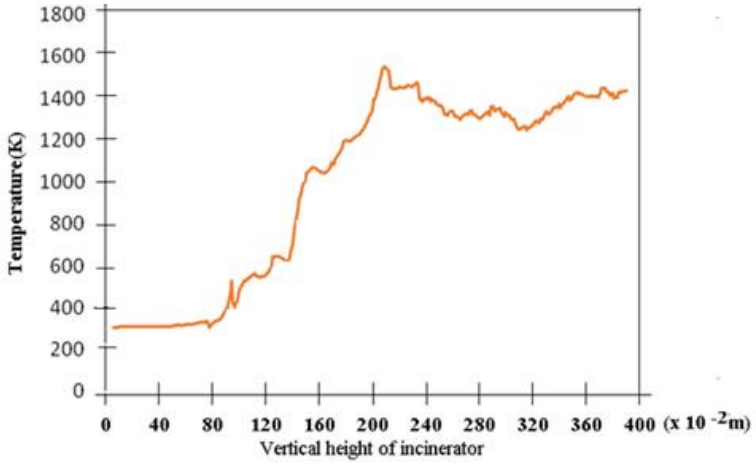

Fig. 13. Temperature variation with incinerator height

Table 4. Validation of simulation results summary

Current model	Input Velocity m/s	Exit gases CO_2(%)	NOx ppm	CO ppm	O_2 (%)	Residence time (s)	Exit Temp (K)
	3.75	7.07	152	46	4.62	1.73	1400
[68,69]	3.3	11	156.5	20	6.12	2.71	1300 and 1800
Deviation	14%	36%	3%	38%	25%	36%	8% -22%
[32]	3.43	N.A	N.A	32.2	6.91	N.A	1420
Deviation	9%	N.A	N.A	30%	33%	N.A	1%

N.A value not available

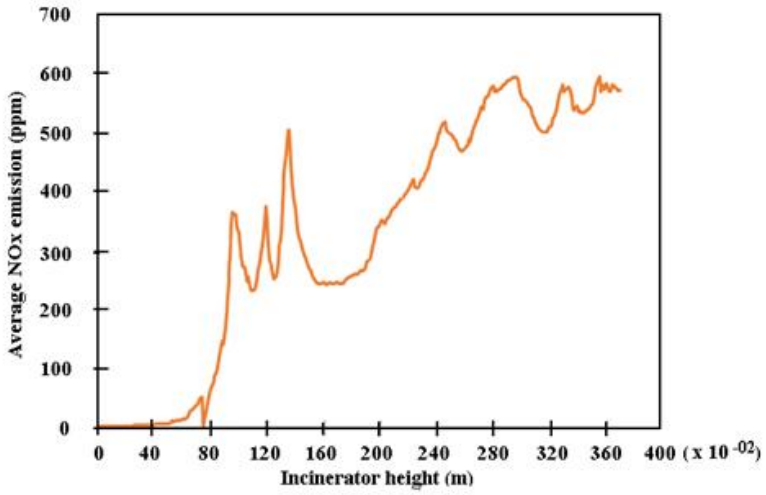

Fig. 54. Average NO_x at incinerator exit of incinerator

3.14.5 Velocity of exit gases

Comparison model result on velocity obtained from the current model and that of [68] it shows good agreements. The model deviation was 14% while the deviation obtained with [32] is 9%.

3.14.6 Exit gas temperature

The comparison of flue gas exit temperature to the current model, with [68]; [32] and [69] shows a good agreement. The high deviation is 22% and lowest is 1%.

4. CONCLUSION

The experimental and simulation study is necessary information for input and operating parameters in optimization of a fixed bed municipal solid waste incineration. The incineration design successfully optimized operating parameters using computational fluid dynamics techniques. The input parameters vary in such a way that the minimum cost of operation and pollution was achieved

DISCLAIMER

The products used for this research are commonly and predominantly use products in our area of research and country. There is absolutely no conflict of interest between the authors and producers of the products because we do not intend to use these products as an avenue for any litigation but for the advancement of knowledge. Also, the research was not funded by the producing company rather it was funded by personal efforts of the authors.

COMPETING INTERESTS

Authors have declared that no competing interests exist.

REFERENCES

1. Swithenbank J, Nassezadeh V, Goh R, Siddall R. Fundamental principles of incinerator design. Developments in Chemical Engineering and Mineral Processing. 1999;7:623-640.
2. Kaschl A, Römheld V, Chen Y. Cadmium binding by fractions of dissolved organic matter and humic substances from municipal solid waste compost. Journal of Environmental Quality. 2002;31:1885-1892.
3. Liang L, Sun R, FEI J, Wu S, Liu X, Dai K, Yao N. Experimental study on effects of moisture content on combustion characteristics of simulated municipal solid wastes in a fixed bed. Bioresource Technology. 2008;99:7238-7246.
4. Sun R, Ismail TM, Ren X, El-Salam MA. Influence of simulated MSW sizes on the combustion process in a fixed bed: CFD and experimental approaches. Waste Management. 2016;49:272-286.
5. Thipse SS, Dreizin EL. Metal partitioning in products of incineration of municipal solid waste. Chemosphere. 2002;46:837-849.
6. Helsen L, Bosmans A. Waste-to-energy through thermochemical processes: matching waste with process. Symposium on Enhanced Landfill Mining. Houthalen-Helchteren, Belgium; 2010.

7. Bidart C, Fröhling M, Schultmann F. Municipal solid waste and production of substitute natural gas and electricity as energy alternatives. Applied Thermal Engineering. 2013;51*:* 1107-1115.
8. Cheng H, Zhang Y, Meng A, Li Q. Municipal solid waste fueled power generation in China: a case study of waste-to-energy in Changchun city. Environmental Science & Technology. 2007;41:7509-7515.
9. Cheng H, Hu Y. Municipal solid waste (MSW) as a renewable source of energy: Current and future practices in China. Bioresource Technology. 2010;101:3816-3824.
10. Yi S, Jang YC, An AK. Potential for energy recovery and greenhouse gas reduction through waste-to-energy technologies. Journal of Cleaner Production. 2018;176: 503-511.
11. Makarichi L, Jutidamrongphan W, Techato KA. The evolution of waste-to-energy incineration: A review. Renewable and Sustainable Energy Reviews. 2018;91: 812-821.
12. Nasserzadeh V, Swithenbank J, Schofield, C, Scott D, Loader A, Leonard A. Design optimization of Coventry municipal solid waste incinerator. Journal of Environmental Engineering. 1994;120: 1615-1629.
13. Pan Y, Wu Z, Zhou J, Zhao J, Ruan X, Liu J, Qian G. Chemical characteristics and risk assessment of typical municipal solid waste incineration (MSWI) fly ash in China. Journal of Hazardous Materials. 2013;261: 269-276.
14. Shin D, Ryu CK, Choi S. Computational fluid dynamics evaluation of good combustion performance in waste incinerators. Journal of the Air & Waste Management Association. 1998;48:345-351.
15. Parkinson AR, Balling R, Hedengren JD. Optimization Methods for Engineering Design, Provo, Utah, USA, Brigham Young University; 2013.
16. Lighty JS, Veranth JM. The role of research in practical incineration systems—A look at the past and the future. Symposium (International) on Combustion. 1998;27:1255-1273.
17. Chen C, Jin YQ, Yan JH, Chi Y. Simulation of municipal solid waste gasification in two different types of fixed bed reactors. Fuel. 2013;103:58-63.
18. Hussain A, Nasir Ani F, Sulaiman N, Fadzil Adnan M. Combustion modelling of an industrial municipal waste combustor in Malaysia. International Journal of Environmental Studies. 2006;63:313-329.
19. Yang W, Nam HS, Choi S. Improvement of operating conditions in waste incinerators using engineering tools. Waste Management. 2007;27:604-613.
20. Kapitler M, Samec N, Kokalj F. Computational Fluid Dynamics Calculations of Waste-To-Energy Plant Combustion Characteristics. Thermal Science. 2011;15:1-16.
21. Anderson SR, Kadirkamanathan V, Chipperfield A, Sharifi V, Swithenbank J. Multi-objective optimization of operational variables in a waste incineration plant. Computers & Chemical Engineering. 2005;29:1121-1130.
22. Mtui PL. Computational analysis of a fixed bed thermal oxidizer for solid wastes disposal. Advanced Materials Research. 2013;699:326-334.
23. Yang Y, Reuter MA, Hartman DT. CFD modelling for control of hazardous waste incinerator. Control Engineering Practice. 2003;11:93-101.
24. Wissing F, Wirtz S, Scherer V. Simulating municipal solid waste incineration with a DEM/CFD method–influences of waste properties, grate and furnace design. Fuel. 2017;206:638-656.
25. Ismail T, El-Salam MA, El-Kady M, El-Haggar S. Three dimensional model of transport and chemical late phenomena on a MSW incinerator. International Journal of Thermal Sciences. 2014;77:139-157.
26. Guo-Hui, Xiao M, Liu Q, Zhao-Sheng Yu. Combustion optimization of municipal solid waste incinerator based on CFD [J]. Journal of South China University of Technology (Natural Science Edition). 2008;2.
27. Koziel S, Yang XS. Computational optimization, methods and algorithms, Chennai, India, Scientific publishing services Pvt. Ltd; 2011.
28. Robinson S. Simulation: The practice of model development and use, London, UK, Palgrave Macmillan; 2014.
29. Shin D, Choi S. The combustion of simulated waste particles in a fixed bed. Combustion and Flame. 2000;121:167-180.

30. Liu Y, Liu Y. Novel incineration technology integrated with drying, pyrolysis, gasification, and combustion of MSW and ashes vitrification. Environmental Science & Technology. 2005;39:3855-3863.
31. Quina MJ, Bordado J, Quinta-Ferreira R. Air pollution control in municipal solid waste incinerators, London, UK, Intechopen Limited; 2011.
32. Huai X, Xu W, Qu Z, Li Z, Zhang F, Xiang G, Zhu S, Chen, G. Analysis and optimization of municipal solid waste combustion in a reciprocating incinerator. Chemical Engineering Science. 2008;63: 3100-3113.
33. Hester RE. Waste treatment and disposal, Cambridge, UK, Royal Society of Chemistry; 2005.
34. Morcos V. Energy recovery from municipal solid waste incineration—A review. Heat Recovery Systems and CHP. 1989;9:115-126.
35. Mudakavi J. Principles and practices of air pollution control and analysis, New-Delhi, India, I.K. International Pvt Ltd; 2010.
36. Kumar SS, Balakrishnan P, Chandraseelan RE. Numerical investigation of swirl enhancement for complete combustion in an incinerator. International Journal of Engineering & Technology. 2014;6:1320-1328.
37. Ujama A, Ebohb F, Chimec T. Effective utilization of a small-scale municipal solid waste for power generation. Journal of Asian Scientific Research. 2013;3:18-34.
38. Mor S, Ravindra K, De Visscher A, Dahiya R, Chandra A. Municipal solid waste characterization and its assessment for potential methane generation: a case study. Science of the Total Environment. 2006;371:1-10.
39. Wu B. Integration of mixing, heat transfer, and biochemical reaction kinetics in anaerobic methane fermentation. Biotechnology and Bioengineering. 2012; 109:2864-2874.
40. Thanh NP, Matsui Y, Fujiwara T. Household solid waste generation and characteristic in a Mekong Delta city, Vietnam. Journal of Environmental Management. 2010;91:2307-2321.
41. Yaghmaeian K, Jaafarzadeh N, Nabizadeh R, Dastforoushan G, Jaafari J. CFD modeling of incinerator to increase PCBs removal from outlet gas. Journal of Environmental Health Science and Engineering. 2015;13:1-6.
42. Frey HH, Peters B, Hunsinger H, Vehlow J. Characterization of municipal solid waste combustion in a grate furnace. Waste Management. 2003;23:689-701.
43. Xia B, Sun DW. Applications of computational fluid dynamics (CFD) in the food industry: A review. Computers and Electronics in Agriculture. 2002;34:5-24.
44. Ansys I. Ansys Fluent User's Guide, California, USA, Ansys Inc; 2015.
45. Fluent I. Fluent 6.3 User's Guide, Beirut, Lebanon, Fluent, Inc; 2006.
46. John R. Howell, Siegel R. Thermal Radiation Heat Transfer, USA, Hemisphere Publishing Cooperation; 1992.
47. Ayaa F. Design of a Municipal Solid Waste Incinerator. Masters degree Dissertation, Makerere University; 2012.
48. Ansys I. ICEM CFD 4.2 Meshing Tutorial manual, California,USA, ICEM CFD Engineering; 2002.
49. Ansys I. Ansys Fluent Users Guide, California, USA, Ansys, Inc; 2009.
50. Surroop D, Mohee R. Power generation from refuse derived fuel. 2nd international conference on environmental engineering and applications, Shanghai, China. IACSIT Press. 2011;242-246.
51. Omari AM, Kichonge BN, John GR, Njau KN, Mtui PL. Potential of municipal Solid Waste, as renewable energy source - a case study of Arusha, Tanzania. International Journal of Renewable Energy Technology Research. 2014;3:1-9.
52. Ayaa F, Mtui P, Banadda N, Van Impe J. Design and computational fluid dynamic modeling of a municipal solid waste incinerator for Kampala city, Uganda. American Journal of Energy Engineering. 2014;2:80-86.
53. Williams PT. Waste treatment and disposal, Chippenham,Wiltshire, UK, John Wiley & Sons; 2013.
54. Reddy PJ. Energy Recovery from Municipal Solid Waste by Thermal Conversion Technologies, CRC Press; 2016.
55. Omari AM, John GR, Njau KN, Mtui PL. Operating Conditions of A Locally Made Fixed-Bed Incinerator, a Case Study of Bagamoyo – Tanzania. *International* Journal of Environmental Monitoring and Analysis. 2015;3:80-90.
56. Ruiz J, Juárez M, Morales M, Muñoz P, Mendívil M. Biomass gasification for electricity generation: Review of current technology barriers. Renewable and

Sustainable Energy Reviews. 2013;18: 174-183.
57. Arena U. Process and technological aspects of municipal solid waste gasification. A review. Waste Management. 2012;32:625-639.
58. Ansys I. Ansys Fluent User's Guide, California, USA, Ansys Inc; 2015.
59. Liang Z, Ma X. Mathematical modeling of MSW combustion and SNCR in a full-scale municipal incinerator and effects of grate speed and oxygen-enriched atmospheres on operating conditions. Waste Management. 2010;30:2520-2529.
60. Ryu C, Shin D, Choi S. Combined simulation of combustion and gas flow in a grate-type incinerator. Journal of the Air & Waste Management Association. 2002;52: 189-197.
61. Urieli I. Engineering Thermodynamics - a graphical approach. 117th ASEE Annual Conference and Exposition. Louisville, Kentucky, USA. American Society for Engineering Education; 2010
62. TSI. Combustion Analysis Basics - An Overview of Measurements, Methods and Calculations Used in Combustion Analysis, Shanghai, China, TSI Incorporated; 2004.
63. Feron P, Hendriks C. CO2 capture process principles and costs. Oil & Gas Science And Technology. 2005;60:451-459.
64. Winter F, Wartha C, Hofbauer H. NO and N2O formation during the combustion of wood, straw, malt waste and peat. Bioresource Technology. 1999;70: 39-49.
65. Chen Y, Ma X, Liao Y, Hu Z, Lin Y, Yu Q. Influence of the interaction on NOx emission during co-combustion of combustible solid waste components. Journal of the Energy Institute. 2016;89: 313-324.
66. CCME. Operating and emission guidelines for Municipal solid waste Incinerators. CCME-TS/WM-TRE003. Ottawa, Canada: Canadian Council of Ministers of the Environment Secretariat; 1989.
67. Nasserzadeh V, Swithenbank J, Scott D, Jones B. Design optimization of a large municipal solid waste incinerator. Waste Management. 1991;11:249-261.
68. Hussain A. CFD Modeling of Grate Furnace Designs for Municipal Solid Waste Combustion. Malaysia; 2012.
69. Lin H, Ma X. Simulation of co-incineration of sewage sludge with municipal solid waste in a grate furnace incinerator. Waste Management. 2012;32:561-567.

Peer-review history:
The peer review history for this paper can be accessed here:
http://www.sdiarticle4.com/review-history/51997